Computational Study of Fish-Shaped Panel with Simultaneously Heaving and Bending Motion

Ruijie Zhu[1], Junshi Wang[2], Haibo Dong[3], Daniel Quinn[4] and Hilary Bart-Smith[5]
Department of Mechanical and Aerospace Engineering
University of Virginia, Charlottesville, VA 22904

Valentina Di Santo[6], Dylan Wainwright[7] and George Lauder[8]
Harvard University, Cambridge, MA 02138

We consider the propulsive performance of an unsteady heaving and bending foil with shape inspired by Thunniform swimmers such as tuna, computationally studying a parameter space of Strouhal Number and phase offsets between heave and bend motions. The phase offset ϕ between the heaving and bending motions proves to be critical in determining the propulsive performance and flow structure of the fish-shaped panel. To maximize thrust, the heave and bend motions have to be almost in-phase but not completely (ϕ ~ 330°), while to maximize efficiency, the bending motion needs to lag the heave motion by about one-fourth of period, which results in a motion of caudal fin at a modest angle of attack, which is similar to biology.

I. Nomenclature

A = trailing edge amplitude
C_L = lift coefficient
C_T = thrust coefficient
c = foil chord
s = foil span
dt = time step
f = frequency of motion
h = leading edge heave position
U_∞ = free stream velocity
St = Strouhal number, $St = 2fA/U_\infty$
α = angle of attack
η = propulsive effieciency, $\eta = C_T/C_P$
θ = pitch angle
ν = kinematic viscosity
ρ = fluid density
ϕ = phase angle between heave and bend motions

[1] Ph.D. Student, AIAA student member, rz6eg@virginia.edu
[2] Ph.D. Student, AIAA student member, jw9un@virginia.edu
[3] Associate Professor, AIAA Associate Fellow, haibo.dong@virginia.edu
[4] Assistant Professor, AIAA member, danquinn@virginia.edu
[5] Professor, hb8h@virginia.edu
[6] Post-doctoral Fellow, vdisanto@fas.harvard.edu
[7] Ph.D. Student, dylan.wainwright@gmail.com
[8] Professor, glauder@oeb.harvard.edu

II. Introduction

In the past, there have been numerous efforts of using a simplified model to study fish swimming. 3-dimensional shape of fish body is often compressed to a 2-dimensional panel with same side view[1-6]; complex kinematics of fish locomotion is often decomposed into sinusoidal heave and pitch motion[7], and flexibility of a composite body is often modeled with linear beam bending models[8]. In many of these cases, the simplified model helps extract key elements of biology that help increase performance or efficiency of fish locomotion compared to traditional artificial propulsion mechanism, such as submarine propeller.

Here we propose a new mechanism we observed[9] in thunniform swimmers that help increase performance, which is bending around peduncle region during swimming. As shown in Fig. 1, the bending happens while the posterior body makes sideway heaving motion, while Fig. 2 shows the phase difference between heaving of posterior body and bending of peduncle joint. The bending of caudal fin is almost out of phase compared to heaving motion of posterior fish body.

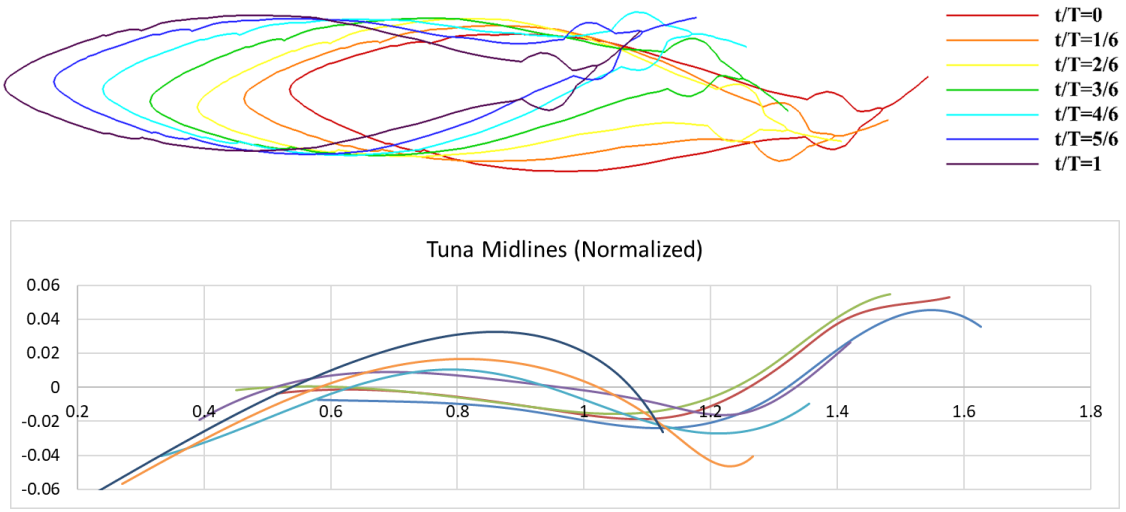

Fig. 1 Thunniform swimming trace/midline kinematics

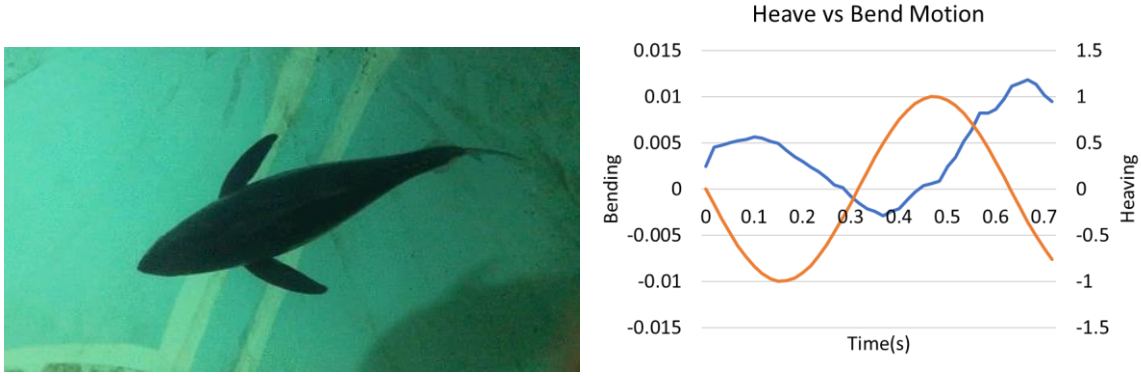

Fig. 2 Phase Relationship between heaving and bending

Motivated by such observations, we present a computational study of a fish-shaped panel with simultaneously heaving and bendig motion. We consider three main questions: do the more complex geometry and kinematics change scaling found in heave and pitch of 2-dimensional airfoil? How does the phase angle affect propulsive performance of the panel? How does the phase angle affect vortex attachment around and wake structure behind the panel?

III. Simulation Methodology

A. Governing Equation and Numerical Method

The fundamental equations used in the simulation are the incompressible Navier-Stokes equations, as:

$$\frac{\partial u_i}{\partial x_i} = 0; \frac{\partial u_i}{\partial t} + \frac{\partial u_i u_j}{\partial x_j} = -\frac{\partial p}{\partial x_i} + \frac{1}{Re}\frac{\partial^2 u_i}{\partial x_j \partial x_j} \tag{1}$$

where the indices, i = 1, 2, 3 represent the x, y and z directions, respectively; p is pressure and u is velocity. The equations are non-dimensionalized with the appropriate length and velocity scales where Re represents the Reynolds number.

A finite -difference based Cartesian grid immersed boundary solver[10] has been developed which allows us to simulate flows with complex geometry. The key feature of this method is that simulations with complex boundaries can be carried out on stationary non-body conformal Cartesian grids, eliminating the need for complicated re-meshing algorithms. The Eulerian form of the Navier-Stokes equations is discretized on a cartesian mesh and boundary conditions on the immersed boundary are imposed through a "ghost-cell" procedure. The code has been verified and applied in many bio-inspired flow-structure interaction cases, such as insects[11–13], bird[13–15] and fish[8, 9], as well as canonical problems. A detailed description of the sharp-interface method and validation of the solver can be found in Ref. [13, 14].

To demonstrate the validity of the CFD solver used in present work, the simulation results of an isolated flapping foil is compared with previously reported experimental results in Fig. 3. In Schnipper's work, the vortex wakes of a symmetricly flapping foil are visualized using a vertically flowing soap film. From 2P wake to 2S wake, the transition of the wakes is described.

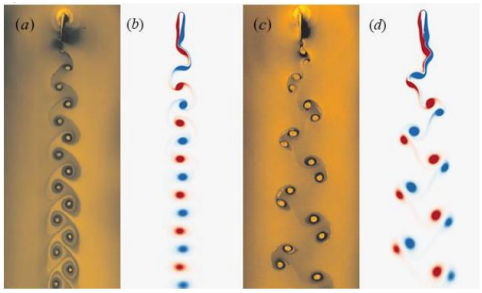

Fig. 3 Comparison of numerical results with experimental data

B. Simulation Setup

The configuration of this study is shown in Fig. 4. It includes a 3-D panel modeled after a tuna tail sample as shown in Fig. 5, with span s = 0.1 m, bending axis in the middle. The anterior part is prescribed with sinusoidal heave motion with amplitude h_0= 0.025 m, while the posterior part has the same heave motion due to joint connection, with an additional pitch motion with amplitude $\theta_0 = 15°$. For the posterior part, the two sinusoidal motions have same frequency of f = 1 Hz, but various phase differences of ϕ = 0° to 270° in intervals of 90°, with a more refined spacing of 30° between 210° and 330° as shown in Table I. In total, the parameter space has 24 simulation cases.

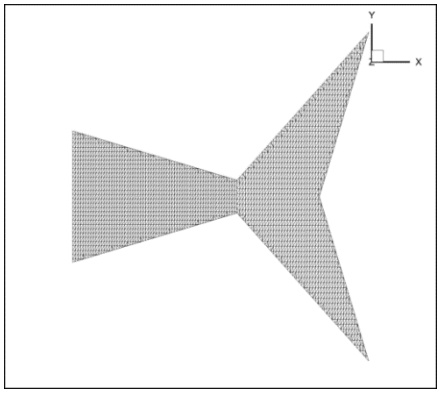

Fig. 4 Mesh of Foil

Fig. 5 Biological sample

The simulations are set to be swimming at fixed location, with 3 different incoming flow speeds of U_∞ = 0.08, 0.12 and 0.16 m/s.

Table I. Case Setup Parameter Space

Parameter	Range
Free Stream Velocity	U_∞ = 0.08, 0.12, 0.16 m/s
Chord	c_1 = 0.05 m, c_2 = 0.04 m
Span	s = 0.1 m
Frequency	f = 1 Hz
Heave Amplitude	h_0 = 0.0125 m
Bend Angle	θ_0 = 15°
Phase Offset	ϕ = 0°, 90°, 180°, 210°, 240°, 270°, 300°, 330°

IV. Simulation Results and Discussion

We present the results on performance in forms of the non-dimensional thrust coefficient, power consumption coefficient, and Froude propulsive efficiency, defined by

$$C_T = \frac{F_x}{\frac{1}{2}\rho U_\infty^2 sc}, C_P = \frac{F_y\dot{h} + M_z\dot{\theta}}{\frac{1}{2}\rho U_\infty^3 sc}, \eta = \frac{C_T}{C_P}.$$

(2)

Time-averaged thrust and power coefficient are denoted by $\overline{C}_T$ and $\overline{C}_P$, while efficiency is always reported as its time-averaged quantity. The foil kinematics are described by the Strouhal number, $St = 2fa_0/U_\infty$, where a_0 is the peak amplitude of the trailing edge motion of caudal fin, and by the reduced frequency, $f^* = fc/U_\infty$.

A. Maximizing Performance through Combined Motion

When pitching motion of caudal fin is added to overall heaving motion of body, the phase offset becomes a critical parameter. Figure 6 illustrates the motion of a fish-shaped foil for phase differences ϕ = 0°, 90°, 180°, 270°. When heave and bend are in phase, the motion to an observer is as if the caudal fin is pitching about some point upstream of its leading edge; when ϕ = 180° the caudal fin appears to pitch about a point behind its leading edge. When ϕ = 90°, the trailing edge of caudal fin leads the leading edge; the system seems to be most "biology-like", having the lowest effective angles of attack. Figure 7 shows performance of the 4 typical cases mentioned above. In summary, we find that the most efficient motions are when φ = 270◦, where the trailing edge lags the leading edge in a slicing motion. In contrast, the highest thrust motions occur when the heaving and pitching motions are nearly in phase, though this comes with a significant loss in efficiency.

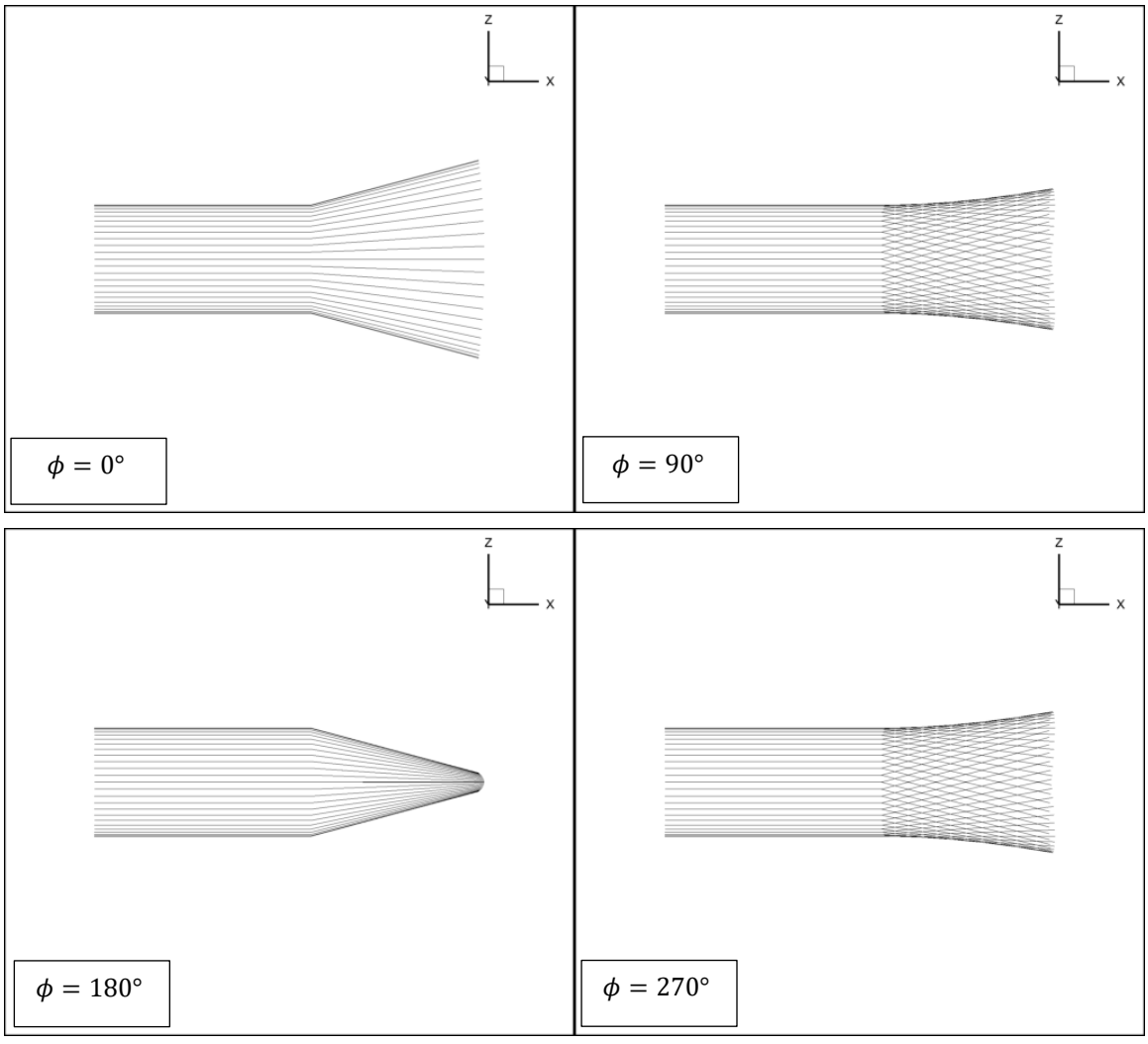

Fig. 6 Kinematics of 4 typical cases

As shown in Fig. 7, variance in flow speed does not affect the trend in terms of effects of phase offset on thrust and efficiency. Given the current resolution of simulation, we observe that peak thrust happens between phase offset of 300° and 330°, while peak efficiency happens around phase offset of 270°.

To better understand the thrust and efficiency performance shown in Fig. 7, we split the power into its lateral force ($F_y\dot{h}$) and moment ($M_z\dot{\theta}$) components. The contributions of the lateral force are similar for both cases, but the moment components differ markedly. When the heave and bending motions are in phase (ϕ = 0°), their accelerations are in phase. Thus, when the caudal fin starts to accelerate laterally, it also accelerates rotationally, working against the resistance of the fluid from lateral motion, yielding a high moment component in the power. However, when heave and bend are offset by ϕ = 270°, the lateral acceleration of the caudal fin produces a force that assists the force associated with bending, thus lowering the moment required. This interaction between the lateral force and moment components of the input power is a critical aspect to achieving the high efficiency we see at ϕ = 270°.

To relate the performance with Strouhal number, we plot efficiency versus Strouhal number in Fig. 8. In contrast to common belief that the optimal efficiency occurs at Strouhal number range of 0.2 – 0.4, there is no significant advantage of Strouhal number being within the optimal range in this specific case. This is mostly due to the fact that when two cases such as ϕ = 90° and 270° share the same Strouhal number due to its definition (shown in Fig. 9), their kinematics at instant time are exactly the opposite.

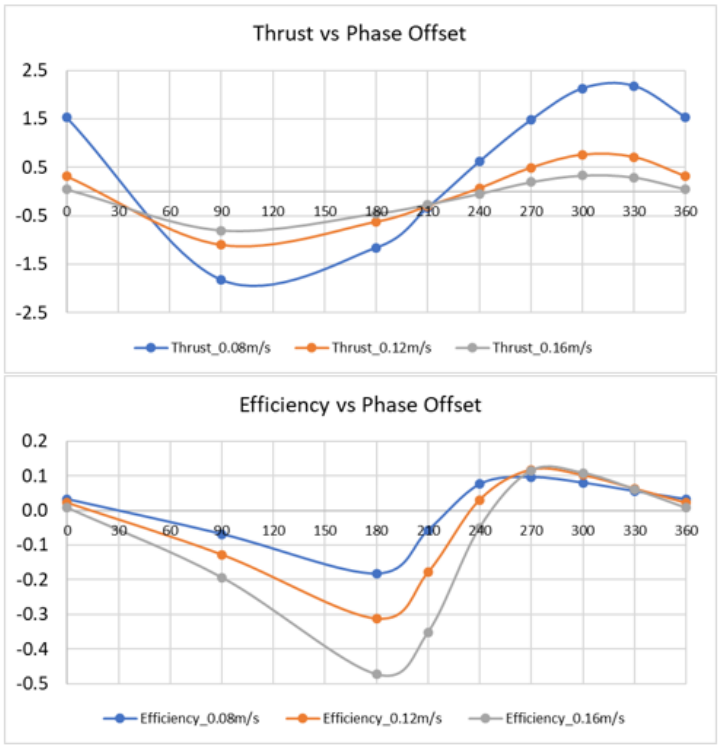

Fig. 7 Coefficient of thrust and efficiency vs phase offset

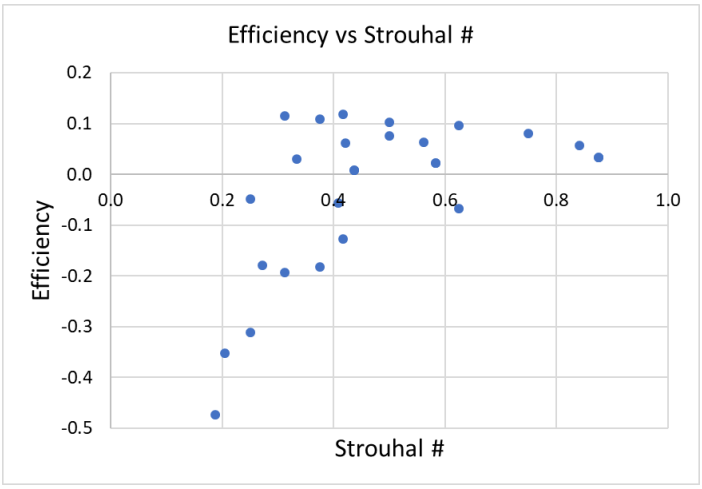

Fig. 8 Efficiency vs Strouhal Number

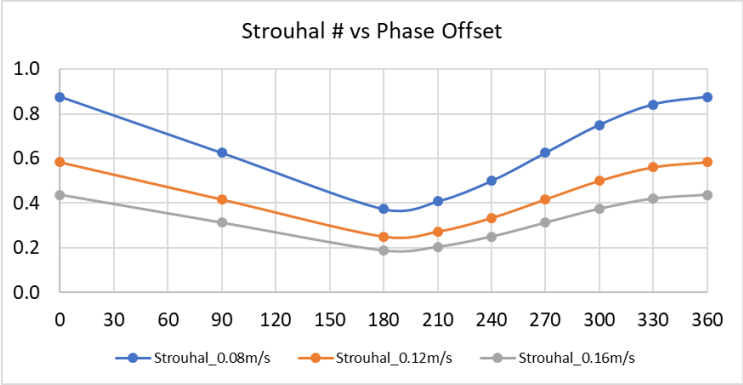

Fig. 8 Strouhal number vs phase offset

B. Wake Dynamics

The wake evolution of optimal efficiency case $\phi = 270°$ is depicted in Fig. 10. We found out in most cases, the vortex shed from the heaving peduncle foil moves downstream and induces a leading-edge vortex for the caudal fin. In the best propulsive performance case, the formed vortex rolls along the foil, which corresponds to the power calculation previously mentioned that bending lagging behind allows the foil to rotate against minimal resistance from water. Similar phenomenon is also observed in simulation of 2D foil with chordwise flexibility[19] and flow tunnel tests of flexible panels[20–24].

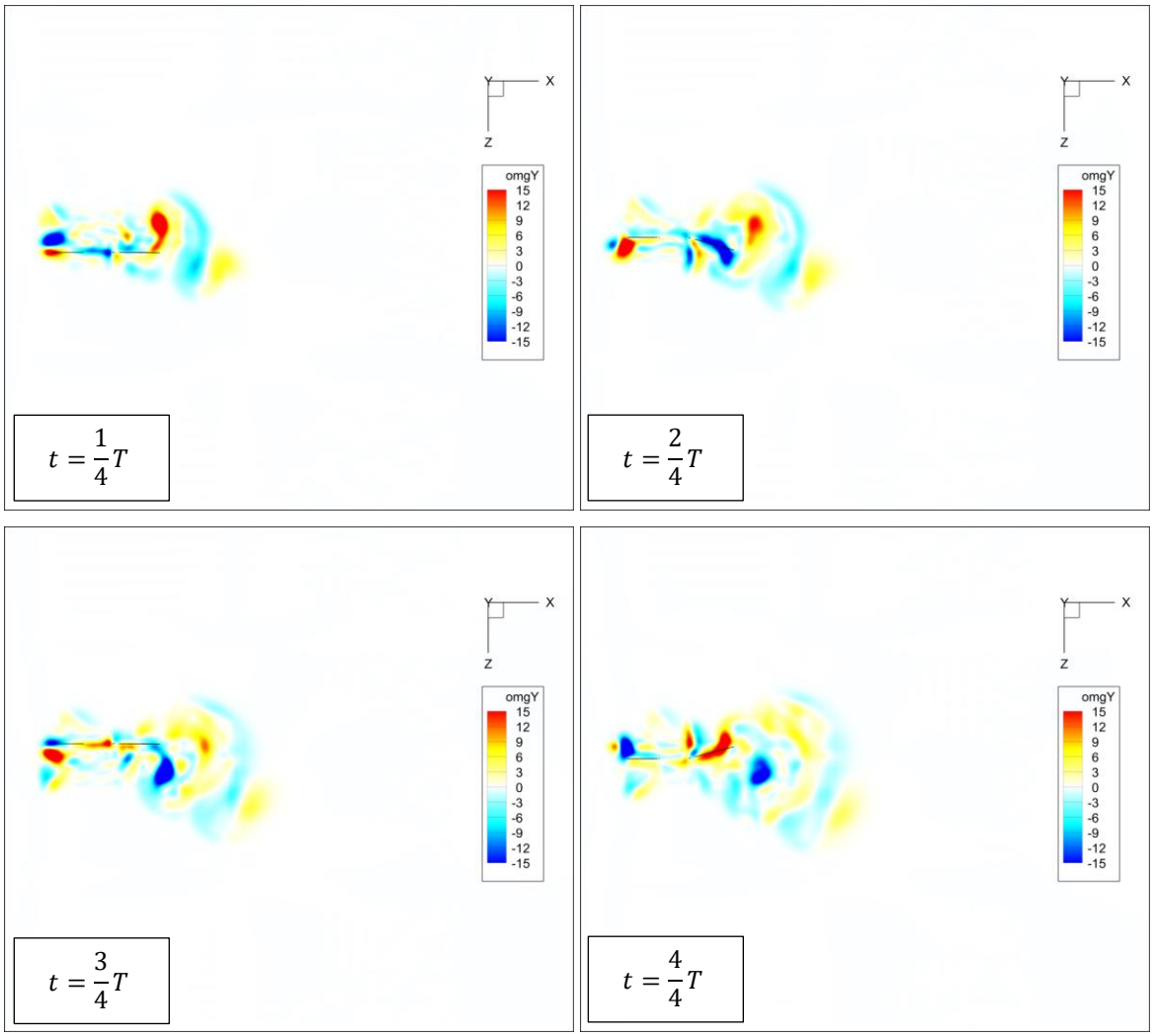

Fig. 10 Streamwise wake dynamics of phase offset ϕ = 270°

Another interesting phenomenon we observed is the spanwise horse shoe vortex ring shown in Fig. 11, caused by the lunate shape of the caudal fin. However, study has shown that this feature does not necessarily help improve performance[25].

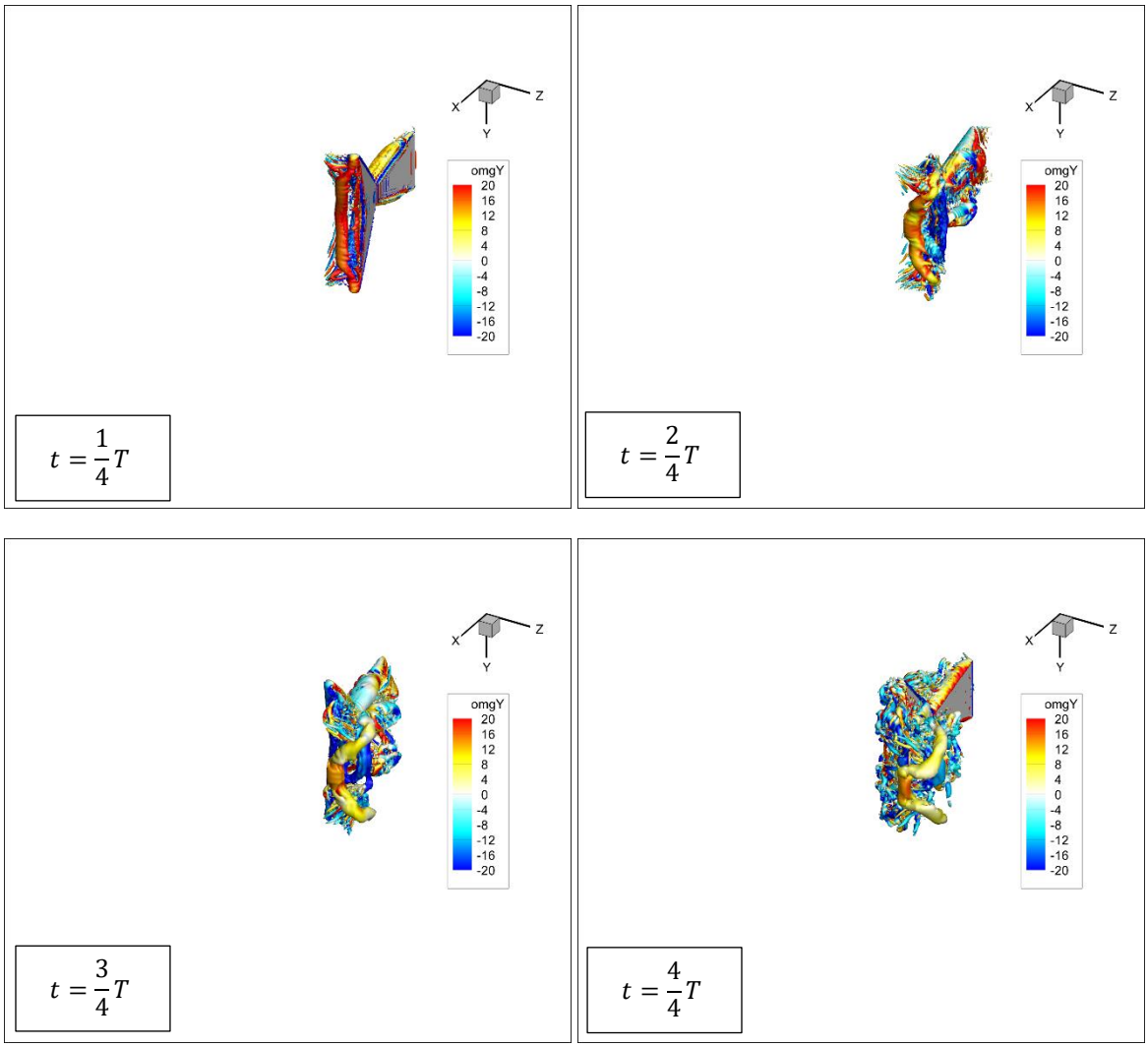

Fig. 11 Wake dynamics of phase offset ϕ = 270°

V. Conclusion

In this study, we present a computational study of the fluid-body interaction of a heave-bend foil. Combining heave and bend motions generally achieves improved performance compared to heave or bend in isolation. A critical parameter is the phase offset between the two motions. Peak thrust occurred near ϕ =330°, while peak efficiency occurred near ϕ=270°, which was coincident with maintaining the smallest peak angles of attack, similar to what we observed in biology.

Further analysis on vortex structure demonstrate the developments of the leading-edge and trailing-edge vortex in streamwise direction, and horse-shoe structure in spanwise direction.

Acknowledgments

This work is supported by ONR MURI grant N00014-14-1-0533 (monitored by Dr Robert Brizzolara) and the David and Lucille Packard Foundation.

References

[1] R. J. Affleck, "Some points in the function, development and evolution of the tail in fishes," *Proc. Zool. Soc. London*, vol. 120, no. 2, pp. 349–368, 1950.

[2] M. J. Lighthill, "Aquatic animal propulsion of high hydromechanical efficiency," *J. Fluid Mech.*, vol. 44, no. 02, p. 265, Nov. 1970.

[3] M. G. Chopra, "Hydromechanics of lunate-tail swimming propulsion," *J. Fluid Mech.*, vol. 64, no. 02, pp. 375–391, Jan. 1974.

[4] G. Karpouzian, G. Spedding, and H. K. Cheng, "Lunate-tail swimming propulsion. Part 2. Performance analysis," *J. Fluid Mech.*, vol. 210, no. 1, p. 329, 1990.

[5] I. Borazjani and M. Daghooghi, "The fish tail motion forms an attached leading edge vortex.," *Proc. Biol. Sci.*, vol. 280, no. 1756, p. 20122071, 2013.

[6] K. L. Feilich and G. V Lauder, "Passive mechanical models of fish caudal fins: effects of shape and stiffness on self-propulsion," *Bioinspir. Biomim.*, vol. 10, no. 3, p. 036002, 2015.

[7] D. Floryan, T. Van Buren, C. W. Rowley, and A. J. Smits, "Scaling the propulsive performance of simultaneously heaving and pitching foils," *J. Fluid Mech.*, vol. 822, pp. 386–397, 2017.

[8] J. L. Tangorra, G. V Lauder, I. W. Hunter, R. Mittal, P. G. a Madden, and M. Bozkurttas, "The effect of fin ray flexural rigidity on the propulsive forces generated by a biorobotic fish pectoral fin," *J. Exp. Biol.*, vol. 213, no. 23, pp. 4043–4054, 2010.

[9] R. Zhu, J. Wang, G. Lewis, J. Zhu, H. Dong, H. Bart-Smith, D. Wainwright, and G. V. Lauder, "Propulsive Performance of Pitching Panels with Bio-Inspired Passive Directional Flexibility," in *47th AIAA Fluid Dynamics Conference*, 2017.

[10] R. Mittal, H. Dong, M. Bozkurttas, F. M. Najjar, A. Vargas, and A. von Loebbecke, "A versatile sharp interface immersed boundary method for incompressible flows with complex boundaries," *J. Comput. Phys.*, vol. 227, no. 10, pp. 4825–4852, 2008.

[11] H. Dong, Z. Liang, H. Wan, C. Koehler, and Z. Gaston, "An Integrated Analysis of a Dragonfly in Free Flight," in *28th AIAA Applied Aerodynamics Conference*, 2010.

[12] G. Liu, H. Dong, and C. Li, "Vortex dynamics and new lift enhancement mechanism of wing-body interaction in insect forward flight," *J. Fluid Mech.*, vol. 795, pp. 634–651, 2016.

[13] M. Xu, M. Wei, C. Li, and H. Dong, "Adjoint-based optimization of flapping plates hinged with a trailing-edge flap," *Theoretical and Applied Mechanics Letters*, vol. 5, no. 1. pp. 1–4, 2015.

[14] Y. Ren, H. Dong, X. Deng, and B. Tobalske, "Turning on a dime: Asymmetric vortex formation in hummingbird maneuvering flight," *Phys. Rev. Fluids*, vol. 1, no. 5, p. 050511, 2016.

[15] Z. Liang, H. Dong, and M. Wei, "Computational Analysis of Hovering Hummingbird Flight," in *48th AIAA Aerospace Sciences Meeting Including the New Horizons Forum and Aerospace Exposition*, 2010.

[16] H. Dong, Z. Liang, and M. Harff, "Optimal Settings of Aerodynamic Performance Parameters in Hovering Flight," *Int. J. Micro Air Veh.*, vol. 1, no. 3, pp. 173–181, 2009.

[17] C. Li, H. Dong, and G. Liu, "Effects of a dynamic trailing-edge flap on the aerodynamic performance and flow structures in hovering flight," *J. Fluids Struct.*, vol. 58, pp. 49–65, 2015.

[18] H. Dong, R. Mittal, and F. M. Najjar, "Wake topology and hydrodynamic performance of low-aspect-ratio flapping foils," *J. Fluid Mech.*, vol. 566, pp. 309–343, 2006.

[19] Q. Zhu, "Numerical Simulation of a Flapping Foil with Chordwise or Spanwise Flexibility," *AIAA J.*, vol. 45, no. 10, pp. 2448–2457, 2007.

[20] P. A. Dewey, B. M. Boschitsch, K. W. Moored, H. A. Stone, and A. J. Smits, "Scaling laws for the thrust production of flexible pitching panels," *J. Fluid Mech.*, vol. 732, pp. 29–46, 2013.

[21] a K. Kancharala and M. K. Philen, "Study of flexible fin and compliant joint stiffness on propulsive performance: theory and experiments.," *Bioinspir. Biomim.*, vol. 9, no. 3, p. 036011, 2014.

[22] R. M. Shelton, P. J. M. Thornycroft, and G. V Lauder, "Undulatory locomotion of flexible foils as biomimetic models for understanding fish propulsion.," *J. Exp. Biol.*, vol. 217, pp. 2110–20, 2014.

[23] D. B. Quinn, G. V Lauder, and A. J. Smits, "Scaling the propulsive performance of heaving flexible panels," *J. Fluid Mech.*, vol. 738, pp. 250–267, 2014.

[24] D. B. Quinn, G. V Lauder, and A. J. Smits, "Maximizing the efficiency of a flexible propulsor using experimental optimization," *J. Fluid Mech.*, vol. 767, no. September, pp. 430–448, 2015.

[25] T. Van Buren, D. Floryan, D. Brunner, U. Senturk, and A. J. Smits, "Impact of trailing edge shape on the wake and propulsive performance of pitching panels," *Phys. Rev. Fluids*, vol. 2, no. 1, p. 014702, 2017.